PCCP

Accepted Manuscript

This article can be cited before page numbers have been issued, to do this please use: R. Credendino, Y. Minenkov, D. Liguori, F. Piemontesi, A. Melchior, G. Morini, M. Tolazzi and L. Cavallo, *Phys. Chem. Chem. Phys.*, 2017, DOI: 10.1039/C7CP04047D.

View Article Online
DOI: 10.1039/C7CP04047D

PCCP

ARTICLE

Accurate Experimental and Theoretical Enthalpies of Association of $TiCl_4$ with Typical Lewis Bases Used in Heterogeneous Ziegler-Natta Catalysis

Received 00th January 20xx,
Accepted 00th January 20xx

DOI: 10.1039/x0xx00000x

www.rsc.org/

R. Credendino,[1] Y. Minenkov,[1] D. Liguori,[2] F. Piemontesi,[2] A. Melchior,[3*] G. Morini,[2] M. Tolazzi[3] and L. Cavallo[1,*]

Abstract. Adducts of $TiCl_4$ with Lewis bases used as internal or external donors in heterogeneous Ziegler-Natta (ZN) catalysis represents a fundamental interaction contributing to the final composition of $MgCl_2$ supported ZN-catalysts. This study presents the accurate experimental evaluation, from titration calorimetry, of the formation enthalpy of $TiCl_4$ adducts with 15 Lewis bases of industrial interests. In addition, we report accurate energies of association of $TiCl_4$ with the same Lewis bases from calculations at the DLPNO-CCSD(T) level of theory. These accurate experimental and theoretical association values are compared with selected methods based on density functional theory (DFT) in combination with popular continuum solvation models. Calculations suggest that the PBE-D3, and M06 functionals in combination with a triple-ζ plus polarization quality basis set provide the best performance when the basis set superposition error (BSSE) is not removed from the association energies. Cleaning the association energies by the BSSE with the counterpoise protocol suggests the B3LYP-D3, TPSS-D3 and M06L as the best performing functionals. Introducing solvent effects with the PCM and SMD continuum solvation models allows comparing the DFT based association enthalpies with the experimental values obtained from titration calorimetry. Both solvation models in combination with the PBE-D3, PBE0-D3, B3LYP-D3, TPSS-D3, M06L, and M06 functionals provide association enthalpies close to the experimental values with MUEs in range 10 – 15 kJ/mol..

Introduction

Polymerization by $MgCl_2$-supported Ziegler-Natta (ZN) catalysts is the most important method in the commercial manufacture of various polymeric materials since 1956.[1,2] Since their discovery, the characterization of ZN catalysts represented a challenge that has been tackled in several experimental[3,4,5,6,7,8,9,10] and theoretical studies.[9,11,12,13,14,15,16] Nevertheless, no clear and conclusive characterization of the active species has been reached yet. The heterogeneous and multisite nature of ZN catalysts certainly contributes to make their understanding and design extremely complicated. The catalytic system active in $MgCl_2/TiCl_4$ promoted ZN polymerization results from the interplay between several components: the basically inert $MgCl_2$ support, $TiCl_4$ that provides the catalytically active metal, the Lewis bases that can be added during catalyst preparation or at polymerization (referred in the literature as internal and external donor, respectively), and the Al-alkyl species that activate the pre-catalyst.[17] The role of the Lewis bases (LB) is particularly remarkable, since their adding is essential to improve stereoselectivity in polypropene synthesis when using supported $MgCl_2/TiCl_4$ ZN catalysts. Choosing opportunely the internal-external donors pair allows to modulate the performance of the catalyst (activity, stereoselectivity) and tune the properties of the resulting polymer (average molecular mass, molecular mass distribution, microtacticity, comonomer distribution). This mixture of ingredients results in a large number of interacting species and the overall behavior of the catalyst will depend on the relative strength of these interactions. This indicates that any comprehensive understanding of ZN catalytic systems requires the accurate knowledge of the interaction energy between the various components.

Additionally, accurate experimental data would provide the unique opportunity to validate the computational chemistry protocols, which are largely used to characterize ZN catalytic systems.[18,19,20,21,22,23] Unfortunately, the reliability of

[1] *King Abdullah University of Science and Technology (KAUST), Physical Sciences and Engineering Division (PSE), KAUST Catalysis Center (KCC), Thuwal, 23955-6900, Saudi Arabia.*
[2] *Basell Italia Srl, G. Natta Research Center, Piazzale G. Donegani 12, 44100 Ferrara, Italy.*
[3] *Dipartimento Politecnico di Ingegneria e Architettura dell'Università di Udine, Laboratori di Scienze e Tecnologie Chimiche, via delle Scienze 99, 33100 Udine, Italy.*

Email: luigi.cavallo@kaust.edu.sa; andrea.melchior@uniud.it
Electronic Supplementary Information (ESI) available: Calorimetry details, Cartesian coordinates, and energies.. See DOI: 10.1039/x0xx00000x

View Article Online
DOI: 10.1039/C7CP04047D

these calculations has always been an open question, not least due to the scarcity of accurate experimental data to be used as reference in benchmark studies. Indeed, one of the most typical approaches consisted in benchmarking density functional theory (DFT) methods versus as accurate wave function based methods, typically at the coupled cluster level with iterative treatment of single and double excitations, and perturbative inclusion of triple excitations, which is abbreviated as CCSD(T) method.[24] However, also this approach is limited by the small size of the systems that can be investigated accurately at the CCSD(T) level, and by the limited size of the basis sets used in these calculations.

Focusing on the interaction between $TiCl_4$ and the LB, the most reliable way to obtain thermochemical data (ΔH values) for metal-ligand complex formation in solution is titration calorimetry.[25] In general, DFT calculations have been shown to be able to reproduce these data in a qualitatively correct way,[25] but the absolute accuracy of the theoretical thermodynamic parameters is often poor (predicted formation constants can be off by few orders of magnitude). This mostly because of the difficulty to correctly take into account factors such as solvation/desolvation processes of the species examined, solvent reorganization and ionic medium effects.[26] In low-polarity non-coordinating solvents these effects are much more limited, so that a closer match between theory and experimental data is in principle expected. This is the case of the complex formation between the Lewis bases and $TiCl_4$, for which accurate thermodynamic data in 1,1,2,2,-tetrachloroethane (TCE) by calorimetric titration were obtained in the past for the Lewis bases shown in Chart 1.[27,28,29]

The Lewis bases of Chart 1 were chosen as representative cases of industrial relevant donors such as ethyl benzoate (**L2**), isobutyl phthalate (**L3**), (2R,3S)-diethyl 2,3-diisopropylsuccinate (**L8**), (2S,3S)-diethyl 2,3-diisopropylsuccinate (**L9**), and 9,9-bis(methoxymethyl)-9H-fluorene (**L15**). Other donors, such as ethyl acetate (**L1**), ortho- meta- and para- diethyl phthalate (**L4**, **L5**, **L6**), diethyl succinate (**L7**), tetrahydrofuran (**L10**), dimethoxyethane (**L11**), dimethoxy propane (**L12**), dimethoxy butane (**L13**), and 3,3-bis-(methoxymethyl)-2,6-dimethylheptane (**L14**), were chosen to explore the influence of (i) different substituent groups, (ii) ring size, (iii) steric effects, and (iv) isomerism on the energetics of the complexation reaction. At the time, a series of DFT methods were employed to reproduce the experimental association energies, and the conclusion was that all the functionals explored clearly underestimated, up 40 kJ/mol, the experimental enthalpies.

Considering that the last 10 years have seen a significant improvement of the DFT functionals, especially in their capability to account for dispersion interactions via either an empirical term (DFT-D methods) or careful tuning of the functional ansatz (e.g. Minnesota functionals), we decided to reinvestigate the same dataset of experimental enthalpies by using contemporary DFT methods. To keep the amount of data to a small number that allows more insightful analysis, we limited this study to the analysis of the performance of only some of the most popular functionals, with a focus on those functionals that have been used in the field of ZN catalysis. Further, considering that the scope of this work is providing a computational protocol that can be applied as routine, we will focus on relatively accurate basis set that can be still applied to systems of up to 100-200 atoms. Since this could undermine the performance of the underlying density functional, test calculations will be performed with extrapolation to complete basis set.

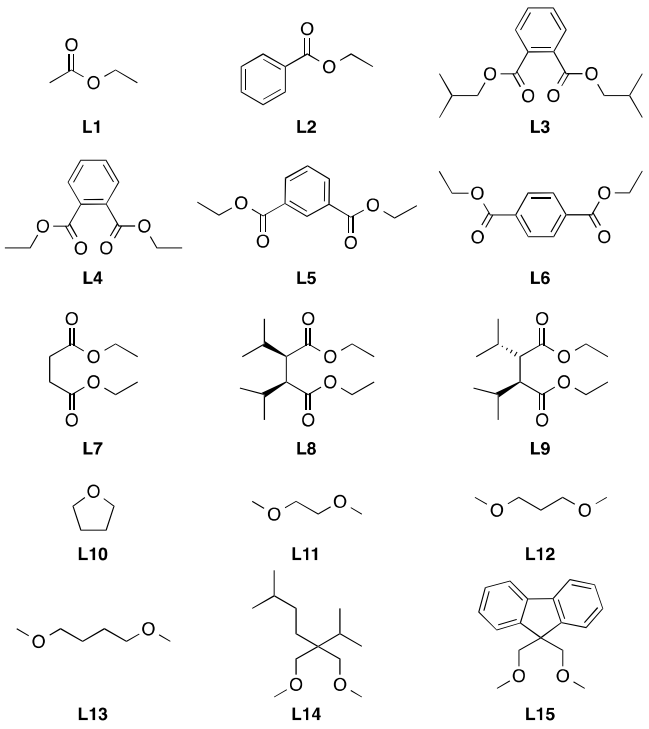

Chart 1. Lewis bases considered in this work.

With the aim to provide a robust experimental reference for evaluating the performance of the DFT functionals, the raw calorimetric data in TCE obtained for previous works[27,29] have been revised with new analysis tools. Moreover, the experiments where the Ti-LB interaction resulted to be weak compared to analogous LBs (namely **L2**, **L5** and **L6**) have been replicated in this work, since even small concentration uncertainties can greatly affect the outcome of calorimetric data analysis.

Further, the interaction energy between $TiCl_4$ and the LBs of Chart 1 was also evaluated in vacuum by using the recently developed domain-based local pair natural orbital coupled cluster theory with single, double, and perturbative triple excitations (DLPNO-CCSD(T)) method.[30] This method has been shown to reproduce the reaction enthalpies involving transition metal complexes[31] and group 1 and 2 metal compounds[32] with an accuracy comparable to the canonical CCSD(T) method. Considering the computational efficiency of the DLPNO-CCSD(T) method, the interaction energies have

View Article Online
DOI: 10.1039/C7CP04047D

been calculated at the complete basis set limit. This allows us to benchmark the tested functionals without including solvent effects.

Experimental details

Solutions of $TiCl_4$ in TCE were prepared from commercial reagents in a glovebox under a controlled atmosphere containing less than 1 ppm of water.

A Tronac model 87-558 precision calorimeter equipped with a 25 mL titration vessel was employed. With respect to the previous experiments[27,29] part of the electronics for data acquisition has been replaced and the titration software was re-designed and integrated in MS-Excel. Both the vessel and the burette were loaded with the reagents, assembled inside the glovebox and then mounted on the calorimeter. The apparatus was calibrated to reproduce the standard enthalpy of neutralization of tris(hydroxymethyl)methylamine (THAM) with 0.1 M HCl (-47.53 kJ/mol).[33] The calorimetric titrations were performed at 298.15 K by adding known volumes of LB solutions (C_{Ligand}= 400 mM, Ligand = **L2**, **L5**, **L6**) to 20 mL of $TiCl_4$ solution in TCE (C_{TiCl4} = 20 mM).

For each titration run, *n* experimental values of the heat produced in the calorimeter vessel ($Q_{ex,j}$, j = 1– *n*) were collected. These values were corrected for the heat of dilution of the titrant ($Q_{dil,j}$), determined in separate runs. The net reaction heats, $Q_{obs,j} = Q_{ex,j} - Q_{dil,j}$ were then used as input data for the data fitting software. The data analysis and revision of previous raw data were carried out using a recently modified version of the MS-Excel tool EST[34] used in combination with Solverstat.[35] These two utilities exploit MS Solver as minimization engine and provide errors on fitted parameters and a series of statistical analyses and tests which are useful when the choice of the speciation models are difficult.

Computational Details

The following popular functionals were tested in this work: the GGA PBE,[36] the hybrid-GGA B3LYP[37] and PBE0[38] the meta-GGA TPSS[39] and M06L,[40] and the hybrid meta-GGA M06,[41] functionals. All the DFT calculations have been carried out with the Gaussian09 package,[42] on the ENEA/CRESCO infrastructure.[43] All structures have been optimized with a triple-ζ plus polarization basis set for main group atoms (TZVP keyword in Gaussian09) and the Stuttgart-Dresden relativistic ECP with the associated triple-ζ basis set for valence electrons (SDD/ECP keyword in Gaussian09),[42] on Ti. Geometry optimizations were performed without symmetry constraints, and the characterization of the located stationary points was performed by analytical frequency calculations. Geometries were optimized using the PBE, PBE0, B3LYP, TPSS, M06L and M06 functionals. Apart from M06L and M06, every functional was tested also with a posteriori inclusion of Grimme's empirical correction term with Becke-Johnson damping to arrive at corresponding DFT-D3 functionals. The dftd3 software was used for these calculations,[44] using the geometry of the corresponding DFT functional.

The impact of the basis set superposition error (BSSE) on the association energies was evaluated using Boys and Bernardi's counterpoise method.[45] Solvent effects, TCE, were evaluated with the PCM and the SMD models, as implemented in Gaussian09 package,[42] through single point calculations on the optimized geometries with inclusion of non-electrostatic terms. As the parameters for TCE solvent have not been implemented in Gaussian09 package, it was decided to employ all parameters but dielectric constant from carbon tetrachloride (CCl_4). The TCE dielectric constant of TCE (2.286) has been used for calculations of electrostatic terms both in PCM and SMD solvation models. Thermodynamic corrections needed to arrive at enthalpies, ΔH_{Corr}(Vacuum), were obtained within ideal gas, rigid rotor and harmonic oscillator approximation. In summary, the absolute enthalpies for all species calculated in this work were obtained as described in Eq. 1

$$H = E_{DFT}(Vacuum) + \Delta H_{Corr}(Vacuum) + \Delta G_{Solv}(TCE) \qquad (1)$$

The total DFT enthalpy of association, ΔH_{DFT}, was calculated using the DFT enthalpies of Eq. 1 as described in Eq. 2:

$$\Delta H_{DFT} = H_{TiCl4/LB} - (H_{TiCl4} + H_{LB}) \qquad (2)$$

Where $H_{TiCl4/LB}$, H_{TiCl4} and H_{LB} are the enthalpies of the optimized $TiCl_4$-LB complex and isolated $TiCl_4$ and LB.

The ORCA suite of programs[46] was employed for the DLPNO-CCSD(T)[30] single-point energy evaluations on the PBE geometries. Tighter than the default "TightPNO" DLPNO settings (TCutPairs = 10^{-5}, TCutPNO = 10^{-7}, and TCutMKN =10^{-3}) were used, as recommended, for applications where the most accurate vales are targeted. The Douglas-Kroll-Hess (DKH2)[47] Hamiltonian was applied as implemented in the ORCA suite of programs since the scalar relativistic effects have been previously shown to affect the reaction energies involving Ti species by 1 – 2 kcal/mol.[48]

The following all-electron triple and quadruple-ζ correlation consistent basis sets re-contracted to be used in conjunction with DKH Hamiltonian were used in the present work. Hydrogen was described with the cc-pVnZ-DK relativistically-contracted basis sets of Dunning.[49] Carbon, and Oxygen were described with the correlation consistent valence cc-pVnZ-DK relativistically contracted basis sets of Dunning.[49] Chlorine atoms were described with the correlation consistent valence cc-pVnZ-DK relativistically contracted basis set of Woon and Dunning.[50] Titanium was described with the correlation consistent core-valence cc-pwCVnZ-DK basis sets of Balabanov and Peterson[51] as the sub-valence electrons of Ti atoms were correlated for better accuracy. The correlation fitting basis sets def2-qzvpp/C developed by Hättig,[52] necessary for the resolution of identity approximation as a part of DLPNO scheme and for the RI approximation as part of double hybrid calculations, were used. All def2/C basis sets were downloaded from the official web page of Turbomole.[53]

To eliminate the effects of basis set incompleteness, we used

View Article Online
DOI: 10.1039/C7CP04047D

the extrapolation schemes for HF and correlation energies of individual species suggested by Helgaker,[54] see Eqs. 3 and 4. For two adjacent triple and quadruple-ζ basis sets:

$$E_{HF}^{n} = E_{HF}^{\infty} + \alpha e^{-1.63n} \quad (3)$$

$$E_{corl}^{n} = E_{corl}^{\infty} + \beta n^{-3} \quad (4)$$

Where n = 3 and 4 for triple and quadruple-ζ basis sets; $E_{HF}^{\infty}/E_{corl}^{\infty}$ HF and correlation energies at the complete basis set (CBS) limit; α/β are parameters to be obtained from a system of the two equations. The total energy at CBS limit with DLPNO-CCSD(T) scheme has been calculated via Eq. 5:

$$\Delta E_{CCSD(T)} = E_{HF}^{\infty}(TiCl_4/LB) + E_{corl}^{\infty}(TiCl_4/LB) - (E_{HF}^{\infty}(TiCl_4) + E_{corl}^{\infty}(TiCl_4) + E_{HF}^{\infty}(LB) + E_{corl}^{\infty}(LB)); \quad (5)$$

The total energy at CBS limit for the PBE and PBE0 functionals was evaluated via equation 6:

$$\Delta E_{DFT} = E_{DFT}^{\infty}(TiCl_4/LB) - (E_{DFT}^{\infty}(TiCl_4) + E_{DFT}^{\infty}(LB)) \quad (6)$$

where E_{DFT}^{∞} has been extrapolated via Eq. 3.
In analogy to the enthalpy of association, the energy of association calculated with the DLPNO-CCSD(T) method, ΔECCSD(T), and the density functionals above, ΔE_{DFT}, was calculated as in Eq. 7:

$$\Delta E_X = E_{TiCl4/LB}(X) - (E_{TiCl4}(X) + E_{LB}(X)), \quad (7)$$

where X = CCSD(T) or DFT.

The performance of the tested DFT functionals versus the experimental enthalpies ΔH° has been evaluated in terms of mean unsigned error (MUE) and mean signed error (MSE), as in Eqs. 8 and 9:

$$MUE = \frac{\sum_{i=1}^{15}|\Delta H_i^0 - \Delta H_i^{DFT}|}{15}, \quad (8)$$

and

$$MSE = \frac{\sum_{i=1}^{15}(\Delta H_i^0 - \Delta H_i^{DFT})}{15}, \quad (9)$$

where 15 is the number of LBs in Chart 1. By definition, MUE can only assume positive values, while MSE can assume negative and positive values, if the specific method has a tendency to underestimate or overestimate the experimental enthalpy, respectively. Similar definition is assumed when the DFT calculated association energies are compared to the DLPNO-CCSD(T) association energies.

Results and Discussion

Calorimetric study. The results of the analysis of the new calorimetric data are reported in Table 1, while in Table S1 the old data are reported for comparison. The plots of new data for Δh_v (= $Q_{obs,j}$/moles of Ti in the titration cell) vs. the moles of LB/ moles of Ti ratio are reported in Figure 1, while the fit of the experimental points of the old data for the other donors are reported in Figures S1a-d (ESI).
In general, the logβ_j and $\Delta H°_j$ values are estimated with a better precision with respect to the previous articles[27,29] with the Letagrop program[55] and a smaller standard deviation is obtained. Small differences in some of the obtained parameters could be due to the different experimental quantity considered by the fitting programs (heat evolved for each data point or the cumulative heat at each addition). Also, some previously estimated stability constants have been here determined (**L7**, **L10**-**L13**, Table 1) and thus also the $\Delta G°_j$ has been calculated.
As TCE is a poorly structured solvent (low polarity, no hydrogen bonds)[56] and no solvent molecules are released from the metal ion upon complexation, the data obtained essentially depend on the strength of the metal-ligand interaction and on the loss of entropy of the reagents. In line with this hypothesis, the reactions are all exothermic with negative $\Delta S°_j$ values.
The most interesting result is the new speciation model obtained by analyzing the new data for the weakly interacting donors (**L2**, **L5**, **L6**). Only the 1:1 TiL species is now sufficient to reproduce correctly the experimental heats, while the previously found TiL_2 complex is always discarded by the fitting procedure (i.e. the logβ_2 tends systematically to zero).
It is interesting to note that **L2**, **L5**, **L6** have similar formation constants (logβ_1 between 1.7 and 1.84) and enthalpies ($\Delta H°_1$ between -57.4 and -62.7 kJ/mol). The $\Delta H°_1$ values are compatible with a monodentate binding when compared with the chelates L3-4 (Table 1). The speciation model implying polynuclear complexes of the type Ti_2L for **L5** and **L6** is also discarded by the fitting procedure, in agreement with diffusion NMR experiments results.[27] The $\Delta S°_1$ values for **L2**, **L5**, **L6** ($\Delta S°_1$ -46.9 - -52.9) are slightly less negative (less unfavorable) with respect to the chelate analogue L3[57]($\Delta S°_1$ -58.1) probably due to the higher internal degrees of freedom of the complex formed with the mono-dentate ligands. The **L3**, **L4**, **L7**, **L8** donors, which are able to coordinate through the carbonyl oxygen, display very close thermodynamic parameters while **L9** has a slightly stronger interaction with $TiCl_4$.
The formation enthalpies for **L1** and **L10** (which are the only two able to form also the 1:2 complex, Figure S1-a and Table 1) show that the ether group binds more strongly $TiCl_4$ with respect to the carbonyl one. This is evident also when the thermodynamic parameters of the di-ethers are compared to those of phthalates and succinates. Moreover, the formation enthalpies and entropies for the complexes of the di-ethers series (**L11**-**L15**) fall in relatively narrow ranges and seem to be modulated by structural factors such as the length of the chain between the oxygens.
It is interesting to note that in the case of **L1** and **L10** the $T\Delta S°_1$ terms (ca. -23 and -35 kJ mol^{-1}) are lower than those of the monodentate **L2**, **L5** and **L6** (average ca. -49 kJ mol^{-1}) and the chelating **L3** and **L4** (ca. -59 kJ mol^{-1}), **L7** and **L9** (ca. -60 kJ mol

View Article Online
DOI: 10.1039/C7CP04047D

^{1}) and **L12** and **L15** (ca. -62 kJ mol^{-1}) donors. Since the decrease of the number of particles is the same in all cases, the less unfavorable entropy of **L1** and **L10** seems to be related to markedly different solvation entropies of these two donors and their complexes with respect to the other monodentate ones (**L2**, **L5** and **L6**). Moreover, the chelating donors present a higher decrease of internal degrees of freedom upon complexation, which is in agreement with their more negative average entropies of complexation.

Table 1. Stability constants ($\log\beta_j$) for the reactions $TiCl_4 + jL \leftrightarrows TiCl_4(L)_j$ in TCE at 298.15 K obtained from the refitting of old raw data[29] and new experiments (a). Thermodynamic parameters ΔG_j°, ΔH_j°, $T\Delta S_j^\circ$ in kJ/mol. Standard deviation reported in parentheses.

Lewis base	j	$\log\beta_j$	ΔG°_j	ΔH°_j	$T\Delta S^\circ_j$
L1	1	3.84(6)	-22.8	-46.02 (1)	-23.2
	2	6.21(6)	-36.5	-95.61(2)	-59.1
L2[a]	1	1.84(1)	-10.5	-57.42 (1)	-46.9
L3	1	4.5(1)	-25.7	-84.63(1)	-58.9
L4	1	4.77(9)	-27.22	-85.33(1)	-58.1
L5[a]	1	1.70(1)	-9.7	-62.66(1)	-52.9
L6[a]	1	1.83(1)	-10.4	-58.69(1)	-48.3
L7	1	4.8(1)	-27.4	-83.39(1)	-56.0
L8	1	4.51(8)	-25.73	-85.10(8)	-59.4
L9	1	5.29(7)	-30.2	-94.28(1)	-64.1
L10	1	4.4(3)	-25.1	-60.0(4)	-35
	2	7.8(3)	-44.5	-118.6(1)	-74
L11	1	>5.5		-103.0	-
L12	1	4.8(1)	-27.4	-89.11(1)	-61.7
L13	1	4.4(1)	-25.1	-88.0	-63.0
L14	1	5.25(6)	-29.9	-96.30(7)	-66.4
L15	1	5.13(1)	-29.3	-86.75(1)	-57.5

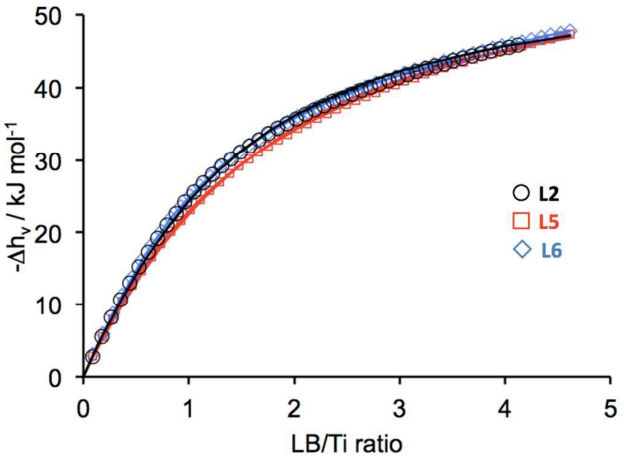

Figure 1. Cumulative molar enthalpy changes per mole of Ti (C_{TiCl4} = 20mM), Δh_v, as a function of the donor/Ti ratio (C_{Ligand} = 400mM). Solid lines are calculated with the $\log\beta_j$ and ΔH°_j values reported in Table 1.

Accurate DLPNO-CCSD(T) association energies. Having established accurate experimental enthalpies of association, ΔH^0, we determined accurate energies of association in vacuum using the DLPNO-CCSD(T) method extrapolated to complete basis set (CBS) limit, ECCSD(T). The calculated association energies, together with the experimental association enthalpies are reported in Table 2. The general trend in the ΔH^0 values is replicated by the ECCSD(T) values.

Assuming that the ΔH^0 values can be written as $\Delta H^0 = \Delta E_{CCSD(T)} + \Delta\Delta H_{corr}(Vacuum) + \Delta\Delta G_{Solv}$, where $\Delta\Delta H_{corr}(Vacuum)$ is the reaction net change of the enthalpic correction and $\Delta\Delta G_{Solv}$ is the reaction net change of the solvation Gibbs free energies of the individual species, we can estimate the impact of these terms on the ΔH^0 values. The $\Delta H_{Corr} + \Delta G_{Solv}$ values reported in Table 2, estimated as $\Delta H_{corr} + \Delta G_{Solv} = \Delta H^0 - \Delta E_{CCSD(T)}$, are usually within 25 kJ/mol in absolute value. Considering the remarkably larger dipole moment of the $TiCl_4$-LB complexes, 10.9±1.6 Debye on average, versus an average dipole moment of 2.4±1.6 Debye of the free LBs, the relatively small $\Delta H_{corr} + \Delta G_{Solv}$ values (essentially due to the change in the geometry of $TiCl_4$ from tetrahedral to octahedral upon complexation and impacting the + ΔG_{Solv} term) indicate a minor role of the solvent in determining the ΔH^0 values.

Having accurate association thermodynamic parameters in vacuum and in solution allows benchmarking the accuracy of various density functionals and of various solvation models. For the sake of discussion, we will start comparing the performance of the tested density functionals in vacuum to reproduce the DLPNO-CCSD(T) values.

Table 2. DLPNO-CCSD(T) association energies, $\Delta E_{CCSD(T)}$, and experimental association enthalpies from Table 1, ΔH^0, and their difference, $\Delta H^0 - \Delta E_{CCSD(T)}$, which can be used to approximate the gas phase enthalpic and solvation correction terms converting $\Delta E_{CCSD(T)}$ to ΔH^0, according to $\Delta H^0 = \Delta E_{CCSD(T)} + \Delta H_{Corr} + \Delta G_{Solv}$. All values in kJ/mol.

Complex	$\Delta E_{CCSD(T)}$	ΔH^0	$\Delta H_{Corr} + \Delta G_{Solv}$
$TiCl_4$-**L1**	-50	-46	4
$TiCl_4$-(**L1**)$_2$	-104	-96	8
$TiCl_4$-**L2**	-43	-57	-15
$TiCl_4$-**L3**	-60	-85	-24
$TiCl_4$-**L4**	-59	-85	-26
$TiCl_4$-**L5**	-42	-63	-21
$TiCl_4$-**L6**	-39	-59	-19
$TiCl_4$-**L7**	-63	-83	-20
$TiCl_4$-**L8**	-81	-85	-4
$TiCl_4$-**L9**	-81	-94	-13
$TiCl_4$-**L10**	-63	-60	3
$TiCl_4$- (**L10**)$_2$	-129	-113	16
$TiCl_4$-**L11**	-78	-103	-25
$TiCl_4$-**L12**	-74	-89	-15
$TiCl_4$-**L13**	-55	-88	-33
$TiCl_4$-**L14**	-78	-96	-19
$TiCl_4$-**L15**	-79	-87	-7

Benchmarking DFT functionals versus DLPNO-CCSD(T) energies. The performance of the various functionals is summarized in Table 3, which reports the mean signed (MSE) and unsigned (MUE) error in reproducing the DLPNO-CCSD(T) energies of association achieved by the different functionals.

View Article Online
DOI: 10.1039/C7CP04047D

As expected, the PBE, PBE0, B3LYP and TPSS functionals, with negative MSE, systematically underestimate the DLPNO-CCSD(T) values. The MUE are in the 20–40 kJ/mol range, with the PBE0 functional resulting in the smallest MUE of 19 kJ/mol, and the B3LYP functional in the largest MUE of 40 kJ/mol. The D3 variant of the same functionals reveals a much better performance of the dispersion-corrected methods, although all of them overestimate the DLPNO-CCSD(T) values. The PBE-D3 functional, with a MUE of only 1 kJ/mol, practically matches the DLPNO-CCSD(T) values, the PBE0-D3 functional, with a MUE of 14 kJ/mol still performs very well, whereas the B3LYP-D and TPSS-D3 functionals, with MUEs of 17 and 24 kJ/mol have mediocre behavior. Moving to the Minnesota functionals, the M06L functional with a MUE of 17 kJ/mol clearly overestimates the DLPNO-CCSD(T) values, meanwhile the M06 functional with a MUE of only 3 kJ/mol demonstrates excellent performance.

Table 3. Mean Signed (MSE) and Unsigned (MUE) Error, in kJ/mol, of the ΔE_{DFT} calculated with different functionals with respect to the DLPNO-CCSD(T) association energy, ECCSD(T), and standard deviation of MUE, σ(MUE). The DFT association energies have not been corrected for the basis set superposition error. The DLPNO-CCSD(T) energies are at the complete basis set limit.

	MSE	MUE	σ (MUE)
PBE	-32	32	11
PBE0	-19	19	8
B3LYP	-40	40	13
TPSS	-21	21	8
PBE-D3	1	1	1
PBE0-D3	14	14	3
B3LYP-D3	17	17	7
TPSS-D3	24	24	9
M06L	17	17	5
M06	0	3	2

For the sake of completeness, we also evaluated the DFT association energies by correcting for the basis set superposition error (BSSE) in the association energies according to the counterpoise (CP) protocol of Boys and Bernardi. The performance of the various functionals is reported in Table 4.

Table 4. Mean Signed (MSE) and Unsigned (MUE) Errors, in kJ/mol, of the ΔE_{DFT} calculated with different functionals with respect to the DLPNO-CCSD(T) association energy, ECCSD(T), and standard deviation of MUE, σ(MUE). The DFT association energies have been corrected for the basis set superposition error through the counterpoise protocol of Boys and Bernardi. The DLPNO-CCSD(T) energies are at the complete basis set limit.

	MSE	MUE	σ (MUE)
PBE	-50	50	16
PBE0	-42	42	14
B3LYP	-59	59	18
TPSS	-41	41	12
PBE-D3	-17	17	6
PBE0-D3	-9	9	4
B3LYP-D3	-2	5	4
TPSS-D3	4	4	6
M06L	-2	3	3
M06	-21	21	7

As expected, correcting for the BSSE reduces the association energies, which results in a decrease of the MSE values by 20 kJ/mol approximately, compare the MSEs values in Tables 3 and 4. Consequently, the PBE, PBE0, B3LYP and TPSS functionals, which do not include a dispersion term, result in stronger underestimation of the DLPNO-CCSD(T) association energies, compared to the BSSE contaminated values. The PBE-D3 and M06 functionals, which were in excellent agreement with the DLPNO-CCSD(T) protocol, clearly underestimate the DLPNO-CCSD(T) values, with MSE close to -20 kJ/mol, while the PBE0-D3, B3LYP-D3 and TPSS-D3 functionals, which were overestimating the DLPNO-CCSD(T) values by approximately 15-20 kJ/mol, are in excellent agreement with the DLPNO-CCSD(T) values after correcting for the BSSE, with MUEs below 10 kJ/mol.

To understand in better details how much the performance of the various functionals depends on the quality of the basis set we estimated the DFT association energies at the CBS limit using the cc-pwCVnZ-DK basis set on Ti and the cc-pVnZ-DK basis set on main group atoms. The MSE/MUE of the PBE and PBE0 functionals amount to -47/47 and -37/37 kJ/mol, which indicates that at the complete basis set limit the PBE and PBE0 functionals still have clear tendency to underestimate the association energies. Inclusion of the dispersion term improves the performance to a MSE/MUE of -14/14 and -4/6 kJ/mol for the PBE-D3 and PBE0-D3 functionals which is practically equal to what was obtained for PBE-D3-CP/TZ and PBE0-D3-CP/TZ methods see Table 4. Comparison with the MSE and MUE values of Tables 3 and 4 indicates that the ΔE_{DFT} at CBS limit are best matched by the ΔE_{DFT} with the TZVP basis set when the BSSE is removed from the energies of association. However, as we will show in the next section, better comparison with the experimental enthalpies of association in solution is achieved when the BSSE is not removed from the calculated enthalpies of association. These results indicate a remarkable influence of the basis set on the performance of the underlying density functional and it indicates that whenever possible CBS calculations should be performed with the PBE0-D3 functional. On the other hand, this protocol can be too much expensive for mechanistic studies on realistic models comprising a large enough $MgCl_2$ cluster to model the support, the active Ti-chloride species with a polymeryl chain and the monomer, and some LBs coordinated to the $MgCl_2$ cluster. Just as an example, the simple $TiCl_4$-**L11** complex requires 305 basis functions with the TZVP basis set, 558 with the cc-pVTZ-DK and 1015 with the cc-pVQZ-DK basis set.

Benchmarking DFT functionals versus calorimetric enthalpies. After the establishment of the performance of the various functionals in vacuum to reproduce accurate DLPNO-CCSD(T) energies, we switch to benchmarking the performance of the

View Article Online
DOI: 10.1039/C7CP04047D

various functionals to reproduce the experimental association enthalpies in solution. The zero-point energy and the thermal contribution to convert the in vacuum energies of association to gas phase enthalpies at 298 K were calculated according to the standard statistical thermodynamics using the ideal gas, rigid rotor and harmonic oscillator approximation. Solvent effects were evaluated according to two models: the PCM model, including the cavitation, repulsion and dispersion non-electrostatic terms, and the SMD model, which by default includes non-electrostatic terms, see Computational Details section. The performance of these two solvation models is reported in Tables 5 and 6, respectively.

Table 5. Mean Signed (MSE) and Unsigned (MUE) Errors, in kJ/mol, of the ΔH_{DFT} calculated with different functionals with respect to the to the experimental ΔH°, and standard deviation of MUE, σ(MUE). Solvent effects included with the PCM continuum solvation model.

	MSE	MUE	σ (MUE)
PBE	-45	45	11
PBE0	-30	30	10
B3LYP	-53	53	11
TPSS	-33	33	6
PBE-D3	-12	12	10
PBE0-D3	3	10	7
B3LYP-D3	4	12	8
TPSS-D3	12	15	14
M06L	7	12	9
M06	-11	13	10

In line with our previous work,[27,28,29] functionals that were not developed to treat dispersion interaction, i.e. PBE, PBE0, B3LYP and TPSS systematically underestimate the experimental ΔH° both with the PCM and the SMD solvation models. The systematic underestimation is confirmed by the negative MSEs. The very large MUEs, in the 30–53 and in the 32-53 kJ/mol range for the PCM and SMD models, respectively, makes any comparison between the different functionals useless. As in the in vacuum calculations, inclusion of dispersion interactions strongly increases the interaction between $TiCl_4$ and the LB improving the agreement with the experimental enthalpies. Thus, the MUEs for all dispersion-corrected functionals are all in range of 10 – 15 kJ/mol. The MUEs calculated for the PBE0-D3, B3LYP-D3, TPSS-D3, M06L functionals and the SMD solvation model turned out to be in exactly the same range of 10-15 kJ/mol range, indicating that both solvation models perform similarly. Analysis of the standard deviations on the MSEs and MUEs values reported in Tables 5 and 6, approximately in the 10-15 kJ/mol range, indicates that all the functionals have similar trends in deviating from the experimental values.

Comparison between the MSE values reported in Tables 5 and 6 indicates that the PCM and SMD models in combination with dispersion-corrected functionals result in final MUEs in association enthalpies in the solvent up to 15 kJ/mol. Considering the amount of the approximations both introduced by us and in the methods used (solvation models, DFT methods, basis sets, etc.) we believe that obtained accuracy is quite good, and practically all the DFT methods corrected for dispersion interactions accomplished with PCM or SMD solvation model can be recommended for calculation of reaction thermochemistry in solution. Also, it has to be stressed that another possible source of errors in our predicted association enthalpies in TCE are due to imperfect treatment of solvent effects both due to approximations introduced by us and due to intrinsic approximations in the solvation models. While the latter can be traced in the original works and reviews on solvation models,[58] we limit ourselves by only listing the approximations introduced by us:

a) As no parameters were available for TCE solvent in Gaussian 09, we have replaced some of them (apart from the dielectric constants) by that of CCl_4.

b) When deriving the absolute enthalpy in solvent through Eq. 1, we used solvation Gibbs free energy instead of the solvation enthalpy, as latter cannot be obtained from any continuum solvation model, mainly, because the temperature dependence of the Gibbs free energy of solvation cannot be reproduced by any continuum solvation model used in the field.[59] However, it was shown that this approximation (replacing ΔH_{Solv} with ΔG_{Solv}) introduces an error of only ca. 1-2 kcal/mol when the reaction enthalpies are considered (due to error cancellation),[59] and is unlikely to be responsible for failures of 30 – 40 kJ/mol.

Table 6. Mean Signed (MSE) and Unsigned (MUE) Error, in kJ/mol, of the $\Delta H°_{DFT}$ calculated with different functionals with respect to the to the experimental ΔH°, and standard deviation of MUE, σ(MUE). Solvent effects included with the SMD continuum solvation model.

	MSE	MUE	σ (MUE)
PBE	-47	47	14
PBE0	-32	32	13
B3LYP	-53	53	15
TPSS	-35	35	9
PBE-D3	-14	15	11
PBE0-D3	1	10	7
B3LYP-D3	4	10	7
TPSS-D3	10	13	8
M06L	3	11	10
M06	-13	15	10

Conclusions

In this work we assessed the capability of a series of computational methods to predict the association energy between $TiCl_4$ and typical Lewis bases used in heterogeneous Ziegler-Natta catalysis. Starting from data published in 2007, experimental reference association enthalpies in solution have been revised or re-determined in TCE. The results are qualitatively confirmed, with the exception of ester **L2** and phthalates **L5** and **L6** for which now only 1:1 species is necessary to fit calorimetric data. In addition, we calculated

View Article Online
DOI: 10.1039/C7CP04047D

accurate in vacuum association energies with the DLPNO-CCSD(T) method. The computational protocols were benchmarked to reproduce both the DLPNO-CCSD(T) association energies in vacuum and the experimental association enthalpies in solution.

The tested computational methods correspond to typical protocols that can be imagined for standard simulations in the field of ZN catalysis. That is, standard functionals capable to handle dispersion interaction, relativistic ECP on the metal, relatively large triple-ζ valence plus polarization basis set, standard inclusion of solvent effects. Overall, these results indicate a remarkable dependence of the computational protocol on the final agreement with accurate energies association in vacuum from DLPNO-CCSD(T) calculations or enthalpies of association in solution from calorimetric titrations. Focusing on the in vacuum calculations, our results indicate that the PBE-D3 and M06 functionals provide MUE from the DLPNO-CCSD(T) values smaller than 5 kJ/mol, and thus can be recommended for accurate calculations. The PBE0-D3, B3LYP-D3 and M06L functionals, with a MUE around 15 kJ/mol, still provide acceptable performance. Correcting the DFT association energies for the basis set superposition error (BSSE) via counterpoise correction scheme drastically changes the performance of the various functionals, with the B3LYP-D3, TPSS-D3 and M06L providing a MUE smaller than 5 kJ/mol, followed by the PBE0-D3 functional with the still acceptable MUE of 9 kJ/mol. All these functionals are thus recommended, with the caveat that the BSSE should be removed from the association energies. The MUE of the PBE-D3 and M06 sharply increases when the BSSE is removed, making this additional step not recommended with these functionals.

Moving to the enthalpies of association in solution, our numbers indicate that both the PCM and SMD solvation models in connection with standard statistical thermodynamics corrections for converting the electronic energy in vacuum to enthalpy in the gas phase at 1 atm, underestimate the experimental association enthalpies. Differently, both PCM and SMD solvation models in connection with the PBE-D3, PBE0-D3, B3LYP-D3, TPSS-D3, M06L, and M06 provides MUE in the acceptable range of 10-15 kJ/mol, and thus are recommended for this kind of calculations.

It remains that the above indications are based on the capability of the different protocols to reproduce the $TiCl_4$ LB interaction. For this reason, for extensive usage in the ZN field the specific functional chosen should be tested towards other properties not investigated in the present work, such as the interaction between $TiCl_4$ and the Lewis bases with the $MgCl_2$ support, and the energetics of monomer coordination/insertion at the Ti-active center.

Acknowledgements

LC and YM thank the King Abdullah University of Science and technology for supporting this work. Computing resources used within this project have been provided by the KAUST Supercomputing Laboratory and by CRESCO/ENEAGRID High Performance Computing infrastructure and its staff.

References

1 G. Natta, in Nobel Lectures in Chemistry, 1963–1970, Elsevier, Amsterdam, The Netherlands 1972, p. 27.

2 K. Ziegler, in Nobel Lectures in Chemistry, 1963–1970, Elsevier, Amsterdam, The Netherlands 1972, p. 6.

3 E. Albizzati, U. Giannini, G. Collina, L. Noristi, L. Resconi, in Polypropylene Handbook, (Ed: E. P. Moore), Hanser, Munich 1996, p. 11.

4 a) P. Brant, A. N. Speca, D. C. Johnston, Magnetic Susceptibility Study of a Model Supported Ziegler-Natta Catalyst: Evidence for Reduced Titanium Clusters, *J. Catal.*, 1988, **113**, 250-255.

5 a) N. Kashiwa, J. Yoshitake, The Influence of the Valence State of Titanium in $MgCl_2$-Supported Titanium Catalysts on Olefin Polymerization, *Makromol. Chem.*, 1984, **185**, 1133-1138. b) N. Kashiwa, A. Toyota, $MgCl_2$ Supported Titanium Catalyst Prepared by Mechanical Pulverization, Polym. Bull., 1984, 11, 471-477.

6 a) T.B. Mikenas, E. I. Koshevoy, V. A. Zakharov, M.I Nikolaeva, Formation of Isolated Titanium(III) Ions as Active Sites of Supported Titanium–Magnesium Catalysts for Polymerization of Olefins, *Macromol. Chem. Phys.,* 2014, **215**, 1707-1720. b) A. G. Potapov, V. V. Terskikh, V.A. Zakharov, G. D. Bukatov, ^{27}Al NMR MAS study of the surface Al complexes formed in reaction of organoaluminium compounds with supported $TiCl_4/MgCl_2$ catalyst, *J. Mol. Catal. A: Chem.,* 1999, **145**, 147-152.

7 a) A. Andoni, J. Chadwick, J. Niemantsverdriet, P. Thüne, The role of electron donors on lateral surfaces of $MgCl_2$-supported Ziegler–Natta catalysts: Observation by AFM and SEM, *J. Catal.,* 2008, 257, 81-86. b) A. Andoni, J. Chadwick, J. Niemantsverdriet, P. Thüne, Investigation of Planar Ziegler-Natta Model Catalysts Using Attenuated Total Reflection Infrared Spectroscopy, *Catal. Lett.,* 2009, **130**, 278-285. c) A. V. Cheruvathur, E. H. G. Langner, J. W. Niemantsverdriet, P. Thüne, In Situ ATR-FTIR Studies on $MgCl_2$-Diisobutyl Phthalate Interactions in Thin Film Ziegler–Natta Catalysts, Langmuir, 2012, **28**, 2643-2651.

8 a) T. Taniike, P. Chammingkwan, V. Q. Thang, T. Funako, M. Terano, Validation of BET specific surface area for heterogeneous Ziegler-Natta catalysts based on αS-plot, *Appl. Catal. A,* 2012, **24**, 437-438. b) (1) H. Mori, M. Yamahiro, M. Terano, M. Takahashi, T. Matsukawa, Lifetime of growing polymer chain in stopped-flow propene polymerization using pre-treated Ziegler catalysts, *Macromol. Chem. Phys.,* 2000, **201**, 289-295. c) S. Poonpong, S. Dwivedi, T. Taniike, M. Terano, Structure–performance relationship for dialkyldimethoxysilane as an external donor in stopped-flow propylene polymerization using a Ziegler–Natta catalyst, *Macromol. Chem. Phys.,* 2014, **215**, 1698-1706.

9 V. Busico, R. Cipullo, G. Monaco, G. Talarico, M. Vacatello, J. C. Chadwick, A. L. Segre, O. Sudmeijer, High-Resolution ^{13}C NMR

View Article Online
DOI: 10.1039/C7CP04047D

Configurational Analysis of Polypropylene Made with $MgCl_2$-Supported Ziegler–Natta Catalysts. 1. The "Model" System $MgCl_2/TiCl_4$–2,6-Dimethylpyridine/$Al(C_2H_5)_3$, *Macromolecules*, 1999, **32**, 4173-4182. b) A. Vittoria, A. Meppelder, N. Friederichs, V. Busico, R. Cipullo, Demystifying Ziegler–Natta Catalysts: The Origin of Stereoselectivity, *ACS Catal.*, 2017, **7**, 4509–4518. c) V. Busico, M. Causa, R. Cipullo, R. Credendino, F. Cutillo, N. Friederichs, R. Lamanna, A. Segre, V. Van Axel Castelli, Periodic DFT and High-Resolution Magic-Angle-Spinning (HR-MAS) ^{1}H NMR Investigation of the Active Surfaces of $MgCl_2$-Supported Ziegler-Natta Catalysts. The $MgCl_2$ Matrix, *J. Phys. Chem. C,* 2008, **112**, 1081. d) E. S. Blaakmeer, G. Antinucci, V. Busico, E. R. H. van Eck, A. P. M. Kentgens, Solid-state NMR investigations of $MgCl_2$ catalyst support, *J. Phys. Chem. C,* 2016, **120**, 6063-6074.

10 A.G. Potapov, V. V. Kriventsov, D. I. Kochubey, G. D. Bukatov, V. A. Zakharov, EXAFS Study of Supported $TiCl_4/MgCl_2$ Catalyst, *Macromol. Chem. Phys.*, 1997, **198**, 3477-3484.

11 M. Boero, M. Parrinello, H. Weiss, S. Hüffer, A First Principles Exploration of a Variety of Active Surfaces and Catalytic Sites in Ziegler-Natta Heterogeneous Catalysis, *J. Phys. Chem. A*, 2001, **105**, 5096-5105.

12 R. Credendino, V. Busico, M. Causa, V. Barone, P. H. M. Budzelaar, C. Zicovich-Wilsone, Periodic DFT modeling of bulk and surface properties of $MgCl_2$, *Phys. Chem. Chem. Phys.,* 2009, **11**, 6525-6532.

13 a) M. Boero, M. Parrinello, K. Terakura, First Principles Molecular Dynamics Study of Ziegler-Natta Heterogeneous Catalysis, J. *Am. Chem. Soc.*, 1998, **120**, 2746-2752. b) M. Boero, M. Parrinello, S. Hüffer, H. Weiss, First Principles Study of Propene Polymerization in Ziegler-Natta Heterogeneous Catalysis, *J. Am. Chem. Soc.*, 2000, **122**, 501-509.

14a) J. Kumawat, V. K. Gupta, K. Vanka, Donor decomposition by Lewis acids in Ziegler-Natta catalyst systems: a computational investigation, Organometallics, 2014, **33**, 4357-4367. b) J. Kumawat, V. K. Gupta, K. Vanka, Effect of donors on the activation mechanism in Ziegler–Natta catalysis: a computational study, *ChemCatChem,* 2016, **8**, 1809-1818.

15 M. Seth, T. Ziegler, Polymerization Properties of a Heterogeneous Ziegler−Natta Catalyst Modified by a Base: A Theoretical Study, *Macromolecules*, 2003, **36**, 6613-6623.

16 a) L. Cavallo, G. Guerra, P. Corradini, Mechanisms of Propagation and Termination Reactions in Classical Heterogeneous Ziegler−Natta Catalytic Systems: A Nonlocal Density Functional Study, *J. Am. Chem. Soc.*, 1998, **120**, 2428-2436.b) R. Credendino, J. T. M. Pater, A. Correa, G. Morini, L. Cavallo, Thermodynamics of formation of uncovered and dimethyl ether-covered $MgCl_2$ crystallites. Consequences in the structure of Ziegler-Natta heterogeneous catalysts, *J. Phys. Chem. C,* 2011, **115,** 13322-13328. c) R. Credendino, J. T. M. Pater, D. Liguori, G. Morini, L. Cavallo, Investigating alkoxysilane coverage and dynamics on the (104) and (110) surfaces of $MgCl_2$-supported Ziegler–Natta catalysts, *J. Phys. Chem. C,* 2012, **116**, 22980-22986. d) R. Credendino, D. Liguori, G. Morini, L. Cavallo, Investigating phthalate and 1,3-diether coverage and dynamics on the (104) and (110) surfaces of $MgCl_2$-supported Ziegler-Natta catalysts, *J. Phys. Chem. C,* 2014, **118**, 8050-8058. e) R. Credendino, D. Liguori, Z. Fan, G. Morini, L. Cavallo, Toward a unified model explaining heterogeneous Ziegler-Natta catalysis, *ACS. Catal.,* 2015, **5**, 5431-5435.

17 E. P. Moore, Jr., Polypropylene Handbook: Polymerization, Characterization, Properties, Applications, Hanser Publishers, Munich 1996.

18 E. Puhakka, T. T. Pakkanen, T. A. Pakkanen, Theoretical Investigations on Ziegler-Natta Catalysis: Models for the Interactions of the $TiCl_4$ Catalyst and the $MgCl_2$ Support, *Surf. Sci.*, 1995, **334**, 289-294.

19 E. Puhakka, T. T. Pakkanen, T. A. Pakkanen, Theoretical Investigations on Ziegler-Natta Catalysis: Alkylation of the $TiCl_4$ Catalyst, *J. Mol. Cat. A: Chemical*, 1997, **120**, 143-147.

20 E. Puhakka, T. T. Pakkanen, T. A. Pakkanen, Theoretical Investigations on Heterogeneous Ziegler−Natta Catalyst Supports: Stability of the Electron Donors at Different Coordination Sites of $MgCl_2$, *J. Phys. Chem. A*, 1997, **101**, 6063-6068.

21 (a) E. Puhakka, T. T. Pakkanen, T. A. Pakkanen, Theoretical Investigations on Ziegler-Natta Catalysis: Coordination of the Electron Donors to Titanium Modified $MgCl_2$ Support, *J. Mol. Cat. A: Chemical*, 1997, **123**, 171-178. (b) E. Puhakka, T. T. Pakkanen, T. A. Pakkanen, E. Iiskola, Theoretical Investigations on Ziegler-Natta Catalysis: Models for the Cocatalyst Components, *J. Organomet. Chem.*, 1996, **511**, 19-27.

22 (a) T. Taniike, M. Terano, Coadsorption Model for First-Principle Description of Roles of Donors in Heterogeneous Ziegler–Natta Propylene Polymerization, *J. Catal.,* 2012, **293**, 39-50. (b) T. Taniike, M. Terano, Coadsorption and Support Mediated Interaction of Ti Species with Ethyl Benzoate in $MgCl_2$ Supported Heterogeneous Ziegler-Natta Catalysts Studied by Density Functional Calculations, *Macromol. Rapid Comm.*, 2007, **28**, 1918-1922. (c) T. Taniike, M. Terano, A Density Functional Study on the Influence of the Molecular Flexibility of Donors on the Insertion Barrier and Stereoselectivity of Ziegler-Natta Propylene Polymerization, *Macromol. Chem. Phys.*, 2009, **210**, 2188-2193.

23 G. Monaco, M. Toto, G. Guerra, P. Corradini, L. Cavallo, Geometry and Stability of Titanium Chloride Species Adsorbed on the (100) and (110) Cuts of the $MgCl_2$ Support of the Heterogeneous Ziegler−Natta Catalysts, *Macromolecules*, 2000, **33**, 8953-8962.

View Article Online
DOI: 10.1039/C7CP04047D

24 A. Correa, N. Bahri-Laleh, L. Cavallo, How Well Can DFT Reproduce Key Interactions in Ziegler–Natta Systems?, *Macromol. Chem. Phys.*, 2013, **214**, 1980−1989.

25 a) F. Endrizzi, P. Di Bernardo, P. L. Zanonato, F. Tisato, M. Porchia, A. A. Isse, A. Melchior, M. Tolazzi, Cu(I) and Ag(I) Complex Formation with the Hydrophilic Phosphine 1,3,5-triaza-7-phosphadamantane in Different Ionic Media. How to Estimate the Effect of a Complexing Medium, *Dalton Trans.*, 2017, **46**,1455-1466. b) F. Endrizzi, A. Melchior, M. Tolazzi, L.F. Rao, Complexation of Uranium(VI) with glutarimidoxioxime: thermodynamic and computational studies, *Dalton Trans.*, 2015, **44**, 13835–13844 c) A. Melchior, E. Peralta, M. Valiente, C. Tavagnacco, F. Endrizzi, M. Tolazzi, Interaction of d^{10} Metal Ions with Thioether Ligands: a Thermodynamic and Theoretical Study, *Dalton Trans.*, 2013, **42**, 6074–6082. d) P. Di Bernardo, P. L. Zanonato, F. Benetollo, A. Melchior, M. Tolazzi, LF. Rao, Energetics and Structure of Uranium(VI)–Acetate Complexes in Dimethyl Sulfoxide, *Inorg. Chem.*, 2012, **51**, 9045–9055.

26 S. Vukovic, B. P. Hay, V. S. Bryantsev, Predicting Stability Constants for Uranyl Complexes Using Density Functional Theory, *Inorg. Chem*, 2015, **54**, 3995–4001.

27 L. Cavallo, J.-M. Ducéré, R. Fedele, A. Melchior, M.C. Mimmi, G. Morini, F. Piemontesi, M. Tolazzi, Ziegler–Natta Catalytic Systems Calorimetric and DFT study on $TiCl_4$-Lewis base interactions, *J. Therm. Anal. Cal.*, 2008, **91**, 101-106.

28 L. Cavallo, R. Fedele, G. Morini, J-M. Ducéré, A. Melchior, A. Correa, F. Piemontesi, M. Tolazzi, An Empirical Correction Term to Density Functional Theory for the Description of the $TiCl_4$-Lewis Base Complexes, *Macromol. Symp.*, 2007, **260**, 122–126.

29 L. Cavallo, S. Del Piero, J-M. Ducéré, R. Fedele, A. Melchior, G. Morini, F. Piemontesi, M. Tolazzi, Key Interactions in Heterogeneous Ziegler−Natta Catalytic Systems: Structure and Energetics of $TiCl_4$−Lewis Base Complexes, *J. Phys. Chem. C*, 2007, **111**, 4412-4419.

30 a) C. Riplinger, F. Neese, An Efficient and Near Linear Scaling Pair Natural Orbital Based Local Coupled Cluster Method, *J. Chem. Phys.*, 2013, **138**, 034106. b) C. Riplinger, B. Sandhoefer, A. Hansen, F. Neese, Natural Triple Excitations in Local Coupled Cluster Calculations with Pair Natural Orbitals., *J. Chem. Phys.*, 2013, **139**, 134101. c) C. Riplinger, P. Pinski, U. Becker, E. F. Valeev, F. Neese, Sparse Maps—A Systematic Infrastructure for Reduced-Scaling Electronic Structure Methods. II. Linear Scaling Domain Based Pair Natural Orbital Coupled Cluster Theory, *J. Chem. Phys.*, 2016, **144**, 024109.

31 a) Y. Minenkov, E. Chermak, L. Cavallo, Accuracy of DLPNO–CCSD(T) Method for Noncovalent Bond Dissociation Enthalpies from Coinage Metal Cation Complexes, *J. Chem. Theory Comput.*, 2015, **11**, 4664-4676. b) Y. Minenkov, E. Chermak, L. Cavallo, Troubles in the Systematic Prediction of Transition Metal Thermochemistry with Contemporary Out-of-the-Box Methods, *J. Chem. Theory Comput.*, 2016, **12**, 1542-1560. c) Y. Minenkov, V. V. Sliznev, L. Cavallo, Accurate Gas Phase Formation Enthalpies of Alloys and Refractories Decomposition Products, *Inorg. Chem.*, 2017, **56**, 1386-1401.

32 Y. Minenkov, G. Bistoni, C. Riplinger, A. A. Auer, F. Neese, L. Cavallo, Pair Natural Orbital and Canonical Coupled Cluster Reaction Enthalpies Involving Light to Heavy Alkali and Alkaline Earth Metals: the Importance of Sub-Valence Correlation, *Phys. Chem. Chem. Phys.*, 2017, **19**, 9374-9391.

33 I. Grenthe, H. Ots, O. Ginstrup, A Calorimetric Determination of the Enthalpy of Ionization of Water and the Enthalpy of Protonation of THAM at 5, 20, 25, 35, and 50 Degrees C., *Acta Chem. Scand.,* 1970, **24**, 1067–1080.

34 S. Del Piero, A. Melchior, P. Polese, R. Portanova, M. Tolazzi, A Novel Multipurpose Excel Tool for Equilibrium Speciation Based on Newton-Raphson Method and on a Hybrid Genetic Algorithm, *Ann. Chim.*, 2006, **96**, 29-49.

35 C. Comuzzi, P. Polese, A. Melchior, R. Portanova, M. Tolazzi, M. SOLVERSTAT: a New Utility for Multipurpose Analysis. An Application to the Investigation of Dioxygenated Co(II) Complex Formation in Dimethylsulfoxide Solution, *Talanta*, 2003, **59**, 67-80.

36 a) J. P. Perdew, K. Burke, M. Ernzerhof, Generalized Gradient Approximation Made Simple, *Phys. Rev. Lett.*, 1996, **77**, 3865-68. b) J. P. Perdew, K. Burke, M. Ernzerhof, Generalized Gradient Approximation Made Simple, Errata, *Phys. Rev. Lett.*, 1997, **78**, 1396-1396.

37 A. D. Becke, Density-Functional Thermochemistry. III. The Role of Exact Exchange, *J. Chem. Phys.*, 1993, **98**, 5648-5652.

38 a) C. Adamo, V. Barone, Toward Reliable Density Functional Methods Without Adjustable Parameters: The PBE0 Model, *J. Chem. Phys.*, 1999, **110**, 6158-69. b) M. Ernzerhof, G. E. Scuseria, Assessment of the Perdew-Burke-Ernzerhof Exchange-Correlation Functional, *J. Chem. Phys.*, 1999, **110**, 5029-36.

39 J.Tao, J. P. Perdew, V. N. Staroverov, G. E. Scuseria, Climbing the Density Functional Ladder: Nonempirical Meta–Generalized Gradient Approximation Designed for Molecules and Solids, *Phys. Rev. Lett.*, 2003, **91**, 146401-4.

40 Y. Zhao, D. G. Truhlar, A New Local Density Functional for Main-Group Thermochemistry, Transition Metal Bonding, Thermochemical Kinetics, and Noncovalent Interactions, *J. Chem. Phys.*, 2006, **125**, 194101-6.

41 Y. Zhao, D. G. Truhlar, The M06 Suite of Density Functionals for Main Group Thermochemistry, Thermochemical Kinetics, Noncovalent Interactions, Excited States, and Transition Elements: Two New Functionals and Systematic Testing of Four M06-class Functionals and 12 Other Functionals, *Theor. Chem. Acc.*, 2008, **120**, 215-41.

View Article Online
DOI: 10.1039/C7CP04047D

42 M. J. Frisch, et al., Gaussian 09, Winnipeg, Connetticut, 2009.
43 G. Ponti, et al. Proceedings of the 2014 International Conference on High Performance Computing and Simulation, HPCS 2014, art. no. 6903807, 1030-1033.
44 S. Grimme, J. Antony, S. Ehrlich, H. Krieg, A consistent and accurate ab initio parametrization of density functional dispersion correction (DFT-D) for the 94 elements H-Pu *J. Chem. Phys.* 2010, **132**, 1541041-19
45 S. F. Boys, F. Bernardi, The Calculation of Small Molecular Interactions by the Differences of Separate Total Energies. Some Procedures with Reduced Errors, *Mol. Phys.*, 1970, **19**, 553.
46 F. Neese, The ORCA Program System, WIREs, *Comput. Mol. Sci.,* 2012, **2**, 73-78.
47 M. Reiher, A. Wolf, Exact Decoupling of the Dirac Hamiltonian. II. The Generalized Douglas–Kroll–Hess Transformation up to Arbitrary Order, *J. Chem. Phys.*, 2004, **121**, 10945-10956.
48 X. Xu, W. Zhang, M. Tang, D.G. Truhlar, Do Practical Standard Coupled Cluster Calculations Agree Better than Kohn–Sham Calculations with Currently Available Functionals When Compared to the Best Available Experimental Data for Dissociation Energies of Bonds to 3d Transition Metals?, *J. Chem. Theory Comput.,* 2015, **11**, 2036−2052.
49 T.H. Jr. Dunning, Gaussian Basis Sets for Use in Correlated Molecular Calculations. I. The Atoms Boron Through Neon and Hydrogen, *J. Chem. Phys.*, 1989, **90**, 1007; W. A. de Jong, R. J. Harrison, D. A. Dixon, Parallel Douglas–Kroll Energy and Gradients in NWChem: Estimating Scalar Relativistic Effects Using Douglas–Kroll Contracted Basis Sets, *J. Chem. Phys.*, 2001, **114**, 48–53.
50 D. E. Woon, T. H. Jr. Dunning, Gaussian Basis Sets for Use in Correlated Molecular Calculations. III. The Atoms Aluminum Through Argon, *J. Chem. Phys.,* 1993, **98**, 1358.
51 N. B. Balabanov, K. A. Peterson, Systematically Convergent Basis Sets for Transition Metals. I. All-Electron Correlation Consistent Basis Sets for the 3d Elements Sc-Zn, *J. Chem. Phys.*, 2005, **123**, 064107.
52 a) C. Hattig, Optimization of Auxiliary Basis Sets for RI-MP2 and RI-CC2 Calculations: Core–Valence and Quintuple-ζ Basis Sets for H to Ar and QZVPP Basis Sets for Li to Kr, *Phys. Chem. Chem. Phys.*, 2005, **7**, 59-66. b) A. Hellweg, C. Haettig, S. Hoefener, W. Klopper, Optimized Accurate Auxiliary Basis Sets for RI-MP2 and RI-CC2 Calculations for the Atoms Rb to Rn, *Theor. Chem. Acc.*, 2007, **117**, 587-597.
53 COSMOLOGIC, http://cosmologic-services.de/basis-sets/basissets.php
54 a) A. Halkier, T. Helgaker, P. Jørgensen, W. Klopper, H. Koch, J. Olsen, A. K. Wilson, Basis-Set Convergence in Correlated Calculations on Ne, N_2, and H_2O, *Chem. Phys. Lett.*, 1998, **286**, 243-252. b) T. Helgaker, W. Klopper, H. Koch, J. Noga, Basis-Set Convergence of Correlated Calculations on Water, *J. Chem. Phys.*, 1997, **106**, 9639-9646. c) A. Halkier, T. Helgaker, P. Jørgensen, W. Klopper, J. Olsen, Basis-Set Convergence of the Energy in Molecular Hartree–Fock Calculations, *Chem. Phys. Lett.,* 1999, **302**, 437-446.
55 R. Arnek, High-speed computers as a supplement to graphical methods. II. Application of LETAGROP to calorimetric titrations *Ark. Kemi*, 1970, **32**, 81-88.
56 Y. Marcus, The Properties of Solvents; John Wiley & Sons, Chichester, England, 1998; Vol. 4.
57 Chelation is Demonstrated by FT-IR Spectra of the Complexes.
58 a) J. Tomasi, M. Persico, Molecular Interactions in Solution: An Overview of Methods Based on Continuous Distributions of the Solvent, *Chem. Rev.*, 1994, **94**, 2027-2094. b) J. Tomasi, B. Mennucci, R. Cammi, Quantum Mechanical Continuum Solvation Models, *Chem. Rev.*, 2005, **105**, 2999-3093. c) A. V. Marenich, C. J. Cramer, D. G. Truhlar, Universal Solvation Model Based on Solute Electron Density and on a Continuum Model of the Solvent Defined by the Bulk Dielectric Constant and Atomic Surface Tensions, *J. Phys. Chem. B*, 2009, **113**, 6378-6396.
59 Y. Minenkov,; G. Occhipinti, V. R. Jensen, Metal−Phosphine Bond Strengths of the Transition Metals: A Challenge for DFT, *J. Phys. Chem. A*, 2009, **113**, 11833–11844.

View Article Online
DOI: 10.1039/C7CP04047D

Material for the Table of Contents

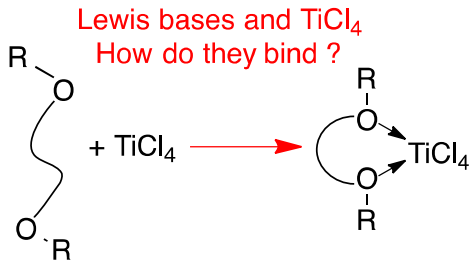

The enthalpy of association of Lewis bases to $TiCl_4$ is analyzed via experimental and computational techniques